

See discussions, stats, and author profiles for this publication at: <https://www.researchgate.net/publication/51522109>

Sensitivity Limit of Rapidly Swept Continuous Wave Cavity Ring-Down Spectroscopy

ARTICLE *in* THE JOURNAL OF PHYSICAL CHEMISTRY A · SEPTEMBER 2011

Impact Factor: 2.69 · DOI: 10.1021/jp111177c · Source: PubMed

CITATIONS

5

READS

30

2 AUTHORS, INCLUDING:



[Kevin Lehmann](#)

University of Virginia

244 PUBLICATIONS 5,864 CITATIONS

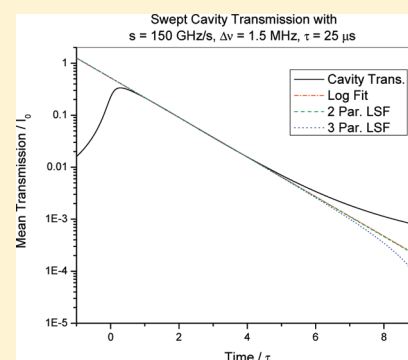
SEE PROFILE

Sensitivity Limit of Rapidly Swept Continuous Wave Cavity Ring-Down Spectroscopy

Haifeng Huang and Kevin K. Lehmann*

Department of Chemistry, University of Virginia, Charlottesville, Virginia 22904-4319, United States

ABSTRACT: The averaged transmitted intensity of a cavity excited by a linearly frequency swept laser with finite line width is derived and presented as a sum over passes, analytical integrals (where the sum of passes is converted to a continuous time variable), and an approximate but computationally more stable stationary phase approximation expression. The transmitted waveform is used to derive the bias in extraction of the cavity decay rate from such a cavity transient for three different fitting models. Numerical simulation of cavity excitation gives statistical fluctuations in the transmitted intensity that leads to noise in the cavity decay rate. For a range of parameters spanning those likely to be encountered in real experiments, numerical results are presented. These demonstrate that the theoretical signal-to-noise ratio and thus sensitivity of swept cavity (or equivalently, frequency) CRDS is substantially below that for CRDS where one attenuates the laser either with current modulation or with an external modulator.



INTRODUCTION

Cavity ring-down spectroscopy (CRDS) has become a widely used method for the detection of weak absorption features in gaseous samples.^{1–6} In this method, sample absorption is detected as an increase in the decay rate of light trapped in a low-loss (high-finesse) optical cavity.¹ While the theoretical shot-noise detection limit of the method has long been known,⁷ the limit appropriate for the more practical case where detector noise dominates has only recently been published.⁸ Our earlier publication calculated theoretical noise levels for a number of variants of the CRDS method and compared them.⁸ One method that we did not then consider is what He and Orr have called swept cavity CRDS.^{9–13} In this method, the length of a high-finesse cavity that contains the sample is swept through resonance with a continuous wave, single frequency laser. This method utilizes the well-known asymmetric ringing decay transient after the sweep^{14–20} to extract the decay time constant τ . Alternatively, the frequency of the laser could be swept because only the relative frequency difference of laser and cavity resonance is important. The equivalence between swept cavity and swept frequency in this method has been discussed in detail by Morville et al.²⁰ In normal continuous wave (cw)-CRDS, the incident laser power is rapidly switched off (relative to the optical cavity decay time) when the cavity transmitted light on the detector exceeds a certain threshold.^{21,22} We have recently published a theoretical and experimental study of how the sensitivity varies with the extinction ratio of the light intensity modulator and found that a very high extinction ratio is needed to reach the sensitivity dictated by the detector (or shot) noise floor.²³ In swept cavity CRDS, the laser intensity is not modulated at all. Rather, the sweep rate is increased to the point that the laser moves through resonance with the cavity in a time short compared to the decay time.^{9,24} Past resonance, the laser is ideally no longer exciting the cavity and thus the light intensity leaving the cavity decays with the

cavity decay rate, as long as the laser does not cross another cavity resonance during this period.

While this method has been proposed several times as a way to determine the cavity decay rate (or equivalently, the finesse),^{15,17–19} or intracavity media gain,²⁵ these previous works have considered an ideal laser with linear frequency sweep but no phase jitter. Li et al.¹⁵ considered the effect of the laser line width, but in an ad hoc way that treats the field amplitude as exponentially decaying (their eq 1). An et al.¹⁷ mentioned the possible effects of laser line width but did not discuss its effects quantitatively. Poirson et al.¹⁸ presented a complete analysis neglecting the effects of laser line width. Morville et al.²⁰ used a phase diffusing laser field, which is equivalent to a laser with finite line width, to model the laser injection of the high-finesse cavity. Hahn et al.²⁴ numerically studied, when the cavity mode is swept through the laser-cavity resonance, how the coupling efficiency between a laser of finite line width and a ring-down cavity changes with scanning rate, laser line width and mirror reflectivity. However, their model and experiments are not consistent with each other, because the model calculates the averaged ringing decay transient with a constant scanning rate, while their experiments measure individual decay transients with the cavity first slowly scanned until the cavity transmission reaches a threshold, then the scan speed rapidly increased. The result of doing that is, the initial decay amplitude is determined by the preset threshold and not by the calculated coupling efficiency. With the initial slow scan rate in their experiments, the transmitted light intensity fluctuates significantly

Special Issue: David W. Pratt Festschrift

Received: November 23, 2010

Revised: June 6, 2011

shot-to-shot, caused by the random phase of the incident laser field if the correlation time of it is shorter than the excitation time.

In this work, we analyze the theoretical sensitivity of this method treating the excitation laser as having a diffusive optical phase, which leads to a Lorentzian laser frequency line shape.^{20,26} This is the dominant source of spectral broadening for distributed feedback (DFB) and Fabry–Perot (FP) diode lasers, which are widely used for CRDS studies. A contribution of such phase diffusion, due to spontaneous emission,²⁶ is present in all lasers but is often overwhelmed by “technical noise” due to acoustic and other fluctuations in cavity length. Our analysis clearly shows that under the experimental conditions reported in literature, the sensitivity of swept cavity CRDS is substantially lower than that of typical cw-CRDS method in which the exciting laser is switched off by a fast modulator.

Following this introduction, we will first introduce the theoretical model, whose efficacy is tested with experimental results. Then we will present the results of numerical simulation to model the phase noise contribution to the noise in the extracted cavity decay rate and discussions. The last part is the conclusion.

■ SWEPT CAVITY CRDS

If one sweeps the frequency of a laser through a cavity resonance fast compared to the cavity decay rate, then one gets a transient response that contains information on the cavity decay rate, or equivalently, finesse. This transient response has appeared in several publications.^{14–18} He and Orr have exploited this effect to build a cw-CRDS instrument that does not require an optical switch.^{9,11–13} We have recently reported that a very high switch extinction ratio (~ 70 dB) is needed for cw-CRDS to realize detector limited sensitivity,²³ and thus this appears to be a significant advantage. In this section, we will present a calculation of the expected signal-to-noise ratio for this cw-CRDS detection method and compare it to the switched laser cw-CRDS method.^{27,28}

Sum-Over-Passes Method. Consider that a laser has a linear frequency sweep, which gives a time dependent electric field $E_L(t)$ of constant amplitude

$$E_L(t) = E_{L0} \exp(-i(\omega_0 t + \pi s t^2 + \phi(t))) \quad (1)$$

where s is the frequency sweep rate (Hz/s) and $\phi(t)$ is the optical phase which is assumed to undergo diffusive motion and is responsible for the laser line width. E_{L0} is the initial laser field amplitude and $i = (-1)^{1/2}$. This equation gives an instantaneous laser angular frequency of $\omega(t) = \omega_0 + 2\pi s t$. For convenience, we take $t = 0$ to be the time at which the laser goes through resonance with the cavity, i.e., $\omega_0 t_r = 2\pi N$, where $t_r = 2L/c$ is the round trip time for light trapped in the cavity and N is an integer. L is the cavity length and c is the speed of light in the cavity. The optical field transmitted through the cavity is

$$E_t(t) = TE_{L0} \sum_{n=0}^{\infty} R^n \exp(-i(\omega_0(t - nt_r) + \pi s(t - nt_r)^2 + \phi(t - nt_r))) \quad (2)$$

where T and R are the power transmission and reflectivity of cavity mirrors, respectively. We assume the two mirrors making the cavity are the same and R and T are real numbers. n is the number of round trips in the cavity. Thus the transmitted intensity $I_t(t) = |E_t(t)|^2$ is

$$I_t(t) = T^2 I_L \sum_{n=0}^{\infty} \sum_{m=0}^{\infty} R^{n+m} \exp(i\omega_0 t_r(n-m) + i2\pi s t t_r(n-m) - i\pi s t_r^2(n^2 - m^2) - i(\phi(t - nt_r) - \phi(t - mt_r))) \quad (3)$$

where $I_L = |E_{L0}|^2$ is the initial incident laser intensity and n, m are the number of round trips. We have implicitly assumed that the cavity is empty. The effect of a sample between the mirrors that obeys Beer's law with absorption coefficient α can easily be included by making the substitutions: $T^2 \rightarrow T^2 \exp(-\alpha L)$ and $R \rightarrow R \exp(-\alpha L)$. The above equation can be evaluated over three regions: $n = m$, $n > m$ and $n < m$. The sum over the first region simply gives a geometric series. The sums over the latter two regions are complex conjugate with each other. Therefore, the transmitted intensity can be written as

$$I_t(t) = \frac{T^2}{1-R^2} I_L + 2T^2 I_L \mathcal{R} \left[\sum_{n=0}^{\infty} \sum_{l=1}^{\infty} R^{2n+l} \exp(-i\omega_0 t_r l - i2\pi s t t_r l + i\pi s t_r^2 l(2n+l) - i(\phi(t - nt_r) - \phi(t - (n+l)t_r))) \right] \quad (4)$$

Here $l = m - n$ for $m > n$ region and $\mathcal{R}[\dots]$ is the real part function.

To calculate the mean intensity (averaged over phase fluctuations of the laser), for a Lorentzian line shape laser, we use the relationship²⁰

$$\langle \exp(-i(\phi(t) - \phi(t'))) \rangle = \exp(-D|t - t'|) \quad (5)$$

with $D = \pi \Delta \nu_L$ and $\Delta \nu_L$ the full width half-maximum (fwhm) of the laser frequency spectrum. For a laser with Gaussian line shape, the relationship is

$$\langle \exp(-i(\phi(t) - \phi(t'))) \rangle = \exp(-\Gamma(t - t')^2) \quad (6)$$

with $\Gamma = (\pi \Delta \nu_L)^2 / (4 \ln 2)$. For this paper, the authors will mainly focus on the situation of Lorentzian line shape because it is more fundamental.

With eq 5, the averaged transmitted intensity as a function of time is

$$\langle I_t(t) \rangle = \frac{T^2}{1-R^2} I_L + 2T^2 I_L \mathcal{R} \left[\sum_{n=0}^{\infty} \sum_{l=1}^{\infty} R^{2n+l} \exp(-i\omega_0 t_r l - i2\pi s t t_r l + i\pi s t_r^2 l(2n+l) - D l t_r) \right] \quad (7)$$

The mean transmitted intensity can be simplified further by summing over index n and using $\omega_0 t_r = 2\pi N$ (N is an integer), giving

$$\langle I_t(t) \rangle = \frac{T^2}{1-R^2} I_L + 2T^2 I_L \mathcal{R} \left[\sum_{l=1}^{\infty} R^l \left(\frac{\exp(i\pi s t_r^2 l^2 - D l t_r)}{1 - R^2 \exp(i2\pi s t_r^2 l)} \right) \exp(-i2\pi s t t_r l) \right] \quad (8)$$

If we do numerical calculation, l can be truncated to $l_{\max} = 10/(-\ln R + D t_r)$. In cw-CRDS experiments, t_r is typically several nanoseconds. Depending on different values of R and D , this l_{\max} is on the order between 10^4 and 10^6 . Therefore, one can easily see that numerical evaluation based on eq 7 is time-consuming because of double summations. On the other hand, evaluation of the expression eq 8 requires evaluation of only l_{\max} terms for each value of time. Note that the term (...) inside the sum is t independent and can be computed once and stored when eq 8 is evaluated for a range of t values. The t -dependent term in the sum forms a geometric series as a function of l and thus requires a single complex multiplication to update. Thus, only $2l_{\max}$ complex multiplications and $2l_{\max}$ additions are required for each

additional time evaluation. This method is exact except for the truncation of the sum process.

When $s = 0$, meaning the laser is centered on the cavity resonance, the above equation gives the mean transmission I_0 ,

$$I_0 = \frac{T^2}{1-R^2} I_L \frac{1+R \exp(-Dt_r)}{1-R \exp(-Dt_r)} \xrightarrow{R \approx 1, Dt_r \ll 1} \left(\frac{T}{1-R} \right)^2 I_L \frac{1}{1+2D\tau} \quad (9)$$

where $\tau = 1/k$ is the cavity decay time and $k = -2 \ln(R)/t_r \approx 2(1-R)/t_r$ is the cavity intensity decay rate. For typical cw-CRDS experiments, those two approximation conditions are naturally satisfied. One of the authors has derived this result previously with another method.²⁷ For Gaussian line width case, this mean transmission of zero scan rate is

$$I_0^G = \frac{T^2}{1-R^2} I_L \left(1 + 2 \sum_{l=1}^{\infty} R^l \exp(-\Gamma t_r^2 l^2) \right) \approx \frac{T^2}{1-R^2} I_L \left[\frac{2}{t_r \Delta \nu_L} \sqrt{\frac{\ln 2}{\pi}} 2^{k^2/(4\pi^2 \Delta \nu_L^2)} \operatorname{erfc} \left(\frac{k \sqrt{\ln 2}}{2\pi \Delta \nu_L} \right) - 1 \right] \quad (10)$$

The approximation results from changing the summation into integration and “erfc” is the complementary error function.

Approximate Integration Method. If $|2\pi s t_r t| \ll 1$, which is equivalent to the condition that the frequency sweep has been much less than one cavity free spectral range, the phase of the field for the different terms in eq 2 have a small change in one round trip time, so it will be a good approximation to convert the sum over passes in the cavity into an integral over time and we get for the transmitted field by the cavity:

$$E_t(t) = \left(\frac{T}{1-R} \right) E_{i,0} \left(\frac{k}{2} \right) \exp(-i\omega_0 t) \int \exp \left(-\frac{k}{2} t_1 - i\pi s(t-t_1)^2 - i\phi(t-t_1) \right) dt_1 \quad (11)$$

For this and following integrals, the domain of integration is always $(0, \infty)$ unless specified. With eq 5, we can calculate the average intensity transmitted by the cavity as a function of time:

$$\langle I_t(t) \rangle = \left(\frac{T}{1-R} \right)^2 I_L \left(\frac{k}{2} \right)^2 \times \int \int \exp \left(-(k/2)(t_1+t_2) + i\pi s((t-t_1)^2 - (t-t_2)^2) - D|t_1-t_2| \right) dt_1 dt_2 \quad (12)$$

For $D = 0$, the two integrals factor (one being the complex conjugate of the other), each integral can be expressed as a complementary error function with a complex argument.¹⁸

$$\langle I_t(t) \rangle \xrightarrow{D \rightarrow 0} \left(\frac{T}{1-R} \right)^2 I_L \left(\frac{k^2}{16s} \right) e^{-kt} \left| \operatorname{erfc} \left(\frac{k + 4\pi i s t}{4\sqrt{-i\pi s}} \right) \right|^2 \approx \left(\frac{T}{1-R} \right)^2 I_L \left(\frac{k^2}{2s} \right) e^{-kt} \quad (13)$$

where \approx refers to estimation of the integral by the stationary phase approximation. The stationary point is $t_1 = t$ and applies when $t \gg 1/(|s|)^{1/2}$, which is the width of the time interval that dominates the integral, i.e., the effective time during which light is

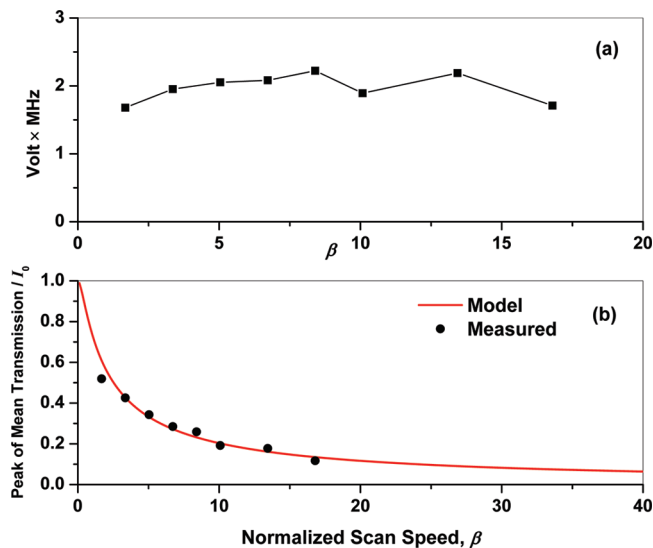


Figure 1. (a) Measured product $s \int_{-\infty}^{\infty} \langle I_t(t) \rangle dt$ vs $\beta = 2\pi s/kD$, the normalized frequency sweep rate.²³ This product is a constant independent of the laser line width $\Delta \nu_L$ and scan speed, s . (b) The curve is the peak value of the mean cavity transmission calculated using eq 15, normalized by $I_0 = (T/(1-R))^2 (1+2\pi\Delta \nu_L \tau)^{-1} I_L$,²⁷ and as a function of β . The dots correspond to the data in (a).

injected into the cavity. This approximation misses the rapid beating in the exact solution, which is due to, mathematically, the sharp cutoff of the integral at $t_1 = 0$ instead of $-\infty$. We note that this explicitly shows that after going rapidly through resonance, the detector power decays, approximately, exponentially with time with the cavity decay rate. He and Orr fit this decay to extract the rate k , starting after the ringing in transmission has decayed away.^{12,13}

The case of exciting a cavity with a frequency swept laser whose phase undergoes diffusion was previously treated by Morville et al.;²⁰ they presented Monte Carlo simulations of phase diffusion to calculate the transmission and average different runs to calculate $\langle I_t(t) \rangle$. Here, we exploit the analytical expression for the field correlation function, represented by eq 5, to provide analytical expressions for the mean transmission in this case. With a finite laser frequency noise ($D > 0$), the double integral in eq 12 no longer factors. If we change integration variables to $x = t_1 - t_2$ and $y = (t_1 + t_2)/2$, with integration domains $(-2y, +2y)$ and $(0, \infty)$ respectively, we can explicitly do the integration over x to give

$$\langle I_t(t) \rangle = \left(\frac{T}{1-R} \right)^2 I_L \left(\frac{k^2}{2D} \right) \int \frac{e^{-ky}}{1 + \left(\frac{2\pi s(y-t)}{D} \right)^2} \left(1 - e^{-2Dy} \left(\cos(4\pi s(y-t)y) - \frac{2\pi s(y-t)}{D} \sin(4\pi s(y-t)y) \right) \right) dy \quad (14)$$

Setting $s = 0$ gives the same approximate I_0 as eq 9. For $D \gg k$, $(2\pi s)^{1/2}$, considering $\exp(-2Dy) \ll 1$ for most of the important part of the integration domain of y , we can neglect the sin and cos terms. In terms of a dimensionless sweep rate, $\beta = 2\pi s/(kD)$, we can write the average transmission as a function of

time relative to passing through resonance as

$$\langle I_t(t) \rangle \xrightarrow{D \gg k, \sqrt{2\pi s}} \left(\frac{T}{1-R} \right)^2 I_L \left(\frac{k}{2D} \right) \int_0^\infty \frac{e^{-u}}{1 + (\beta(u - kt))^2} du \quad (15)$$

The factor in front of the integral is an approximation of I_0 in eq 9 under the condition $D \gg k$. The integral can be evaluated in terms of the imaginary part of the exponential $n = 1$ integral with complex argument,

$$\int \frac{e^{-u}}{1 + (\beta(u - kt))^2} du = \frac{e^{-kt}}{\beta} \mathcal{I}(E_1(-i\beta^{-1} - kt) \exp(-i\beta^{-1})) \quad (16)$$

Alternatively, the integral can be evaluated numerically as the integrand is monotonic and can be expressed as a recursion relationship with the integral evaluated only over an interval of the size of the time step. Note that the transmission is reduced by a factor that depends only on the reduced frequency sweep rate, β , and the reduced time, kt . The reduced time corresponding to the peak of $\langle I_t(t) \rangle$ is 1 for $\beta \ll 1$ and approaches zero for $\beta \gg 1$, with a value of 0.5 for $\beta = 1.5$. The peak cavity transmission is smaller than that of the unswept laser by a factor that approaches unity as $\beta \rightarrow 0$, is 0.5 for $\beta = 2.5$ and slowly $\rightarrow \pi/\beta$ for $\beta \gg 1$. The dependence of peak $\langle I_t(t) \rangle$ on β is calculated and shown by the curve in Figure 1b.

It is not easy to measure this peak value directly from the averaged cavity transmission waveform on a scope. The main difficulty comes from an excess low-frequency jitter of the laser frequency relative to the cavity resonance.²³ This makes it hard to determine the time zero at which the laser is on-resonant with the cavity for each transmitted waveform. Therefore, we used an indirect method to obtain this peak value.

Starting from eq 12, we can calculate the quantity $s \int_{-\infty}^{\infty} \langle I_t(t) \rangle dt$ by using

$$\int_{-\infty}^{\infty} \exp(-i2\pi xt) dt = \delta(x) \quad (17)$$

with $\delta(x)$ the Dirac δ function and x a variable. It is found this quantity is

$$s \int_{-\infty}^{\infty} \langle I_t(t) \rangle dt = \left(\frac{T}{1-R} \right)^2 \frac{k}{4} I_L \quad (18)$$

This conclusion is correct for both Lorentzian and Gaussian line shapes, and surprisingly, the constant is independent of the laser line width $\Delta\nu_L$, as well as the frequency sweep rate s . Previously we have derived eq 18 from eq 15, which is an approximation for $D \gg k$ case.²³ This means the time integration of the sin and cos terms in eq 14 is equal to zero.

Figure 1a displays the measured product $s \int_{-\infty}^{\infty} \langle I_t(t) \rangle dt$ versus β . It clearly shows the product $s \int_{-\infty}^{\infty} \langle I_t(t) \rangle dt$ is a constant. This result has been published before and one can find details of the measurement in our previous paper.²³ For the $D \gg k$ case, this quantity $\approx I_0 D/2$. The semiconductor diode laser we used has a short-term (approximately millisecond) line width of 1 MHz.²³ The decay time constant τ (or $1/k$) of our cavity is 221 μ s. This gives an I_0 about 1.3 V (here and at certain places later, I_0 has been transformed to the voltage output of a detector). On the other hand, the laser frequency jitter does not affect the time

integration of $\langle I_t(t) \rangle$. Therefore, combining with eq 15 ($D \gg k$), we can deduce the peak value of the mean transmission of different frequency sweep rates. The data points in Figure 1b were obtained by this method and they match the calculated curve very well.

The calculation of $\langle I_t(t)^2 \rangle$, for $D \gg k$ and $(2\pi s)^{1/2}$, will reduce to a pair of products of two integrals that are each $\langle I_t(t) \rangle$ (as above for the unswept case), so we again have χ^2 with 2 degrees of freedom intensity fluctuations. This can be rationalized because in the frequency swept case, the cavity is excited for an effective time of $\sim 1/(2\pi s)^{1/2}$ and if this is many coherence times of the laser, $1/D$, we expect the central limit theorem result to apply. For the very rapid sweep case, $2\pi s \gg D^2$, then eq 14 is dominated by the last term and we get a result that is independent of D , as we would expect because in this limit we are exciting the cavity for an effective time that is short compared to the dephasing time of the laser. Note that for $D \sim 10^7 \text{ s}^{-1}$ as appropriate for single mode diode lasers, $2\pi s = D^2$ means a sweep rate of 1.6 THz/s, more than 2 orders of magnitude higher than we use in our experiments. For external cavity diode lasers, however, $D \sim 10^4 \text{ s}^{-1}$ applies (see below), so then the same swept rate would put one in this very rapid sweep limit where the phase noise of the laser causes only minor fluctuations in cavity transmission.

Upon examination of eq 14, it is evident that $\langle I_t(t) \rangle$ does not decay exponentially at long time, but rather decays as an inverse second power. Physically, this is explained by the fact that the laser with random phase diffusion has a Lorentzian spectral density distribution and the tail of this Lorentzian continues to excite the cavity after the intensity injected while passing through resonance has decayed away. Our analysis assumed that the laser was close to resonance with the cavity. If the laser frequency shift is more than one-half of the free spectral range, $FSR = 1/\tau_r$, then the intensity will begin increasing instead of decreasing. In this limit, the integral expression is not a good approximation and one must use the sum of passes expression instead. This thus puts a practical limit on the size of the sweep rate that can be used $\sim s \leq kFSR/10 = (1/10)(1-R)(c/2L)^2$. Even this is perhaps an overestimate as it assumes perfect mode matching and thus one does not have to consider the laser passing through resonance of higher transverse modes, which will also distort the transmitted intensity transient. If one is working with a nearly concentric or nearly planar symmetric cavity, then the low orders of higher transverse modes are closely spaced on one frequency side of the TEM₀₀ modes and proper choice of scan direction will mean they cross resonance before the main mode. However, both these are nearly unstable optical cavities and thus alignment sensitivity is high. For a cavity deep in the stable regime, the higher order transverse mode spacing is on the order of half the FSR and the sweep rate needs to be carefully selected so that no transverse modes with significant excitation are crossed during the time period that the cavity transmission is fitted to extract a decay rate.

For $D\tau$ not $\gg 1$, the highly oscillatory terms in eq 14 can make a significant contribution, but numerical integration of these terms is very difficult. They can be estimated by noting that there are two regions of the integration variable y that can be expected to make the dominant contribution. One is $y \sim t/2$, where the phase of the sin and cos terms has a stationary point. The second is $y \sim t$, where the factor $(1 + \beta^2(y - t)^2)^{-1}$ is strongly peaked. Rather surprisingly, we find that the contribution of the sin and cos terms cancel in this region. The stationary phase

approximation applied to the first region gives contribution

$$\int \frac{e^{-ky}}{1 + \left(\frac{2\pi s(y-t)}{D}\right)^2} \left[-e^{-2Dy} \left(\cos(4\pi s(y-t)y) - \frac{2\pi s(y-t)}{D} \sin(4\pi s(y-t)y) \right) \right] dy$$

$$\approx \frac{D^2 e^{-(k+2D)|t|/2}}{D^2 + (\pi s t)^2} \frac{1}{\sqrt{4s}} \left[\frac{\pi s t}{D} \sin(\pi(st^2 - 1/4)) - \cos(\pi(st^2 - 1/4)) \right] \quad (19)$$

Numerical calculations show that the stationary phase approximation reproduces the phase and local frequency of the oscillations but tends to overestimate their size by a factor that increases with time t . One needs to be careful when this approximated equation is used. Equation 19 generates ringing for both $t > 0$ and $t < 0$ sides of $\langle I_t(t) \rangle$ while eq 14 correctly gives ringing only for $t > 0$ side. Further numerical calculations show that when t is in the range between 0 and the first positive zero point of the ringing, eq 19 gives large error. The reasons are as follows. First, for $t \approx 0$, the stationary point of sin and cos terms and the peak point of the factor $(1 + \beta^2(y-t)^2)^{-1}$ are getting close to each other; second, the integration domain of y is $(0, \infty)$. The combination of both breaks the cancellation of the sin and cos terms.

Monte Carlo Simulation Method. In swept CRDS, the decay transients are averaged a number of times before fitting to an exponential curve. The above two methods calculate this mean transmission through the ring-down cavity. This averaged transmission waveform can be used to predict the bias of swept CRDS method, but not the noise level, which is determined by the fluctuations in the fitted cavity decay rate. We have derived an integral expression for the transmitted intensity-transmitted intensity correlation function, $\langle \delta I(t_1) \delta I(t_2) \rangle$, and this can be used to derive an analytical expression for the standard error in k .²³ However, this analytical result involves a six-dimensional integral with a rapidly oscillating integrand and is very difficult to numerically evaluate. As an alternative, we have numerically simulated a large number of sweeps using essentially the same Monte Carlo method as Moreville et al.²⁰ for generating a phase diffusing laser field input to the cavity. Here we present two ways of doing this simulation: one is exact but more time-consuming in calculation; the other is approximate but has higher calculation efficiency.

With eq 2, we can derive an iteration equation for calculating the transmitted field:

$$E_t(t) = RE_t(t - t_r) + TE_{L0} \exp(-i\omega_0 t - i\pi s t^2 - i\phi(t)) \quad (20)$$

with a time step of round trip time t_r . Because $\omega_0 t_r = 2\pi N$, the term $\exp(-i\omega_0 t)$ is a constant phase for times separated by multiples of t_r and can be included in $\phi(t)$. A reasonable initial condition of this iteration is $E_t(t_s) = TE_{L0} \exp(-i\pi s t_s^2 - i\phi(t_s))$, which corresponds to turning on the input laser at this time. $\phi(t)$ undergoes a random walk with $\phi(t_s + (j+1)t_r) = \phi(t_s + jt_r) + \varepsilon_j$, where ε_j is a Gaussian random number with mean zero and standard deviation $(2\pi\Delta\nu_L t_r)^{1/2}$. For each step, the transmitted light intensity is $I_t(t) = |E_t(t)|^2$. Therefore, each vector of $\phi(t)$ with a length of total time points will generate one single transmitted waveform, part of which (possibly after averaging several simulated decay transients) is fitted to an exponential decay for decay rate k extraction. In CRDS experiments, the k is proportional to the absorbance of the sample contained inside the cavity and fluctuations in the extracted k values is

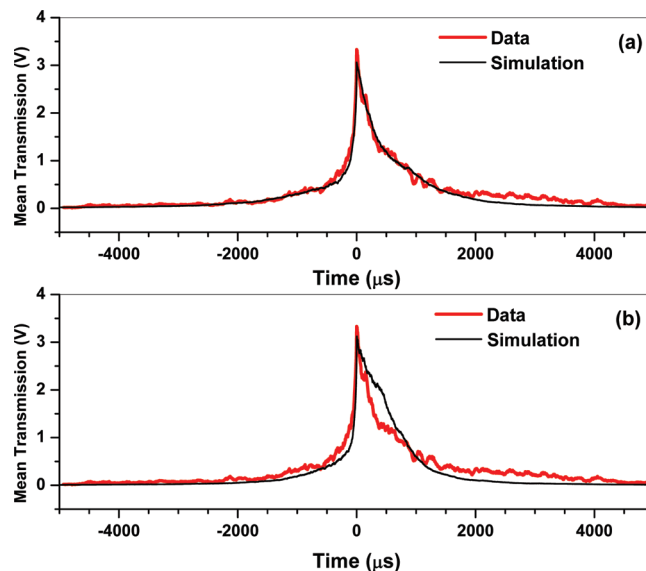


Figure 2. Averaged waveform and simulation for $s = 0.76$ GHz/s: (a) $\Delta\nu_L = 1.0$ MHz; (b) $\Delta\nu_L = 0.5$ MHz. Waveform trigger threshold is 3 V. The thick curve is experimental data, and the thin one is simulation.

proportional to the effective noise in the absorbance of the sample. With many of this single sweep transients, we can simulate both the bias and uncertainty of the swept CRDS method. Numerical simulation is started with an empty cavity when the laser frequency is $10\Delta\nu_L$ below resonance with the cavity and continued until the time t_f where the laser frequency is either $10\Delta\nu_L$ or 8τ above resonance (whichever is larger). In cavity ring-down experiments, the round trip time t_r is typically on the order of nanoseconds; hence the total number of time steps for each sweep is more than $100k$ if $\tau = 25 \mu s$. In spite of being computationally demanding, this should be an accurate simulation of a swept CRDS experiment when using a DFB or other laser for which phase diffusion dominates.

We can also start with eq 11 to derive a similar iteration relation with larger time step δt . The integration step size, δt , is the smaller of $0.2/\pi\Delta\nu_L$ and $(0.1/(\pi s))^{1/2}$. At time t , the input optical field has phase $\pi s t^2 + \phi(t)$, and $\phi(t)$ under goes a random walk with $\phi(t_{j+1}) = \phi(t_j) + \delta_j$ where δ_j is a Gaussian random number with mean zero and standard deviation $(2\pi\Delta\nu_L \delta t)^{1/2}$. Integration over time interval δt treating ϕ and the laser frequency as constant over this interval gives the following recursive relationship,

$$E(t_{j+1}) = e^{-k\delta t/2} E(t_j) + \left[\frac{T}{1-R} (k/2) E_{L0} e^{-\pi i s t_j^2 - 2\pi i s t_j \delta t} \frac{1 - \exp((-k/2 + 2\pi i s t_j) \delta t)}{0.5k - 2\pi i s t_j} \right] e^{-i\phi(t_{j+1})} \quad (21)$$

Note that the term in [...] is constant for different realizations of a given simulation (i.e., different sets of $\phi(t_j)$) and thus was calculated once and stored. This equation is equivalent to eq 20 if $R \approx 1$ and $2\pi s t_j \delta t \ll 1$. If δt is not larger than t_r , there is no advantage to using this approximate method.

To test eq 21, we have made a comparison between the measured mean cavity transmission waveforms and the simulated ones. When those waveforms were recorded, the cavity length scan range was more than half of the laser wavelength and the

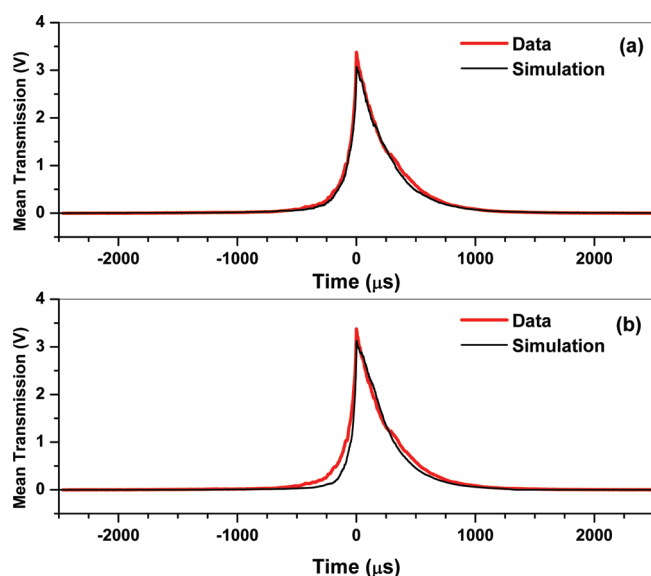


Figure 3. Averaged waveform and simulation for $s = 3.8$ GHz/s: (a) $\Delta\nu_L = 1.0$ MHz; (b) $\Delta\nu_L = 0.5$ MHz. Waveform trigger threshold is 3 V. The thick curve is experimental data, and the thin one is simulation.

cw-CRDS setup was not triggered to record ring-down transients when the DFB diode laser and the ring-down cavity were on-resonant with each other. Therefore, the incident laser intensity was not turned off as in usual CRDS experiments, hence cavity transmission waveforms were generated noninterruptedly. To avoid the difficulty in determining the cavity-laser resonant moment caused by laser frequency jitter discussed previously, only the waveforms whose maximum amplitude is greater than the trigger threshold (set to 3 V) of the scope were recorded, and they were averaged with time zero point defined as the trigger moment. Those with maximum amplitude smaller than 3 V were not triggered by the scope. In this way, we have recorded some cavity transmission waveforms for two sweep rates: 51 waveforms for sweep rate 0.76 GHz/s and 100 waveforms for 3.8 GHz/s. These two averaged waveforms are compared with the simulated ones from eq 21, which were also filtered for sufficient peak transmission and shifted in time to align the trigger point. Parameters used in the simulation include:²³ mirror transmission $T = 2.4 \times 10^{-6}$, mirror reflectivity $R = 0.999\,994$, cavity lifetime $\tau = 221$ μ s, laser line width $\Delta\nu_L = 1.0$ MHz, and two sweep rates. From Figure 1, $I_0 = 1.3$ V. Therefore, the ratio between the trigger threshold and I_0 is $3\text{ V}/1.3\text{ V} = 2.31$, which is also used in the simulation.

Figures 2a and 3a display the comparison between data and simulation. We find they match very well. One of the key parameters in the simulation is $\Delta\nu_L$, which has been previously measured to be 1.0 MHz for short-term (approximately milliseconds) with near Lorentzian shape by a homodyne method (with a time delay of 33 μ s).²³ The rising edge of the simulated waveform depends strongly on $\Delta\nu_L$, providing a convenient way to measure the relevant laser spectral width. In the simulation, a smaller (0.5 MHz) laser line width will give a steeper rising edge than was measured, and a larger (1.5 MHz) line width the opposite. As an example, Figures 2b and 3b show the results of simulations with the same parameters except with $\Delta\nu_L = 0.5$ MHz (correspondingly, the ratio between the trigger threshold and I_0 reduced by a factor of 2). For the correct 1 MHz line width,

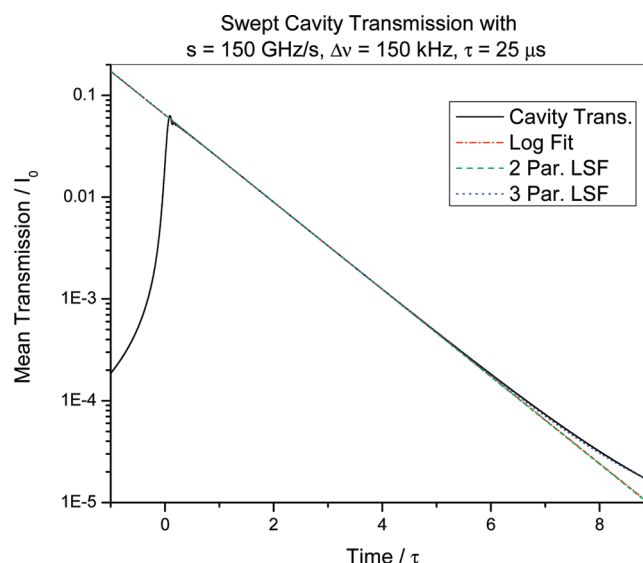


Figure 4. Calculated frequency swept mean cavity transmission, normalized to the mean transmission of $s = 0$, I_0 . The sweep rate is 150 GHz/s, the excitation laser has a fwhm line width of 150 kHz, and the cavity has a decay time of 25 μ s. The fitting range is $1-4.5\tau$.

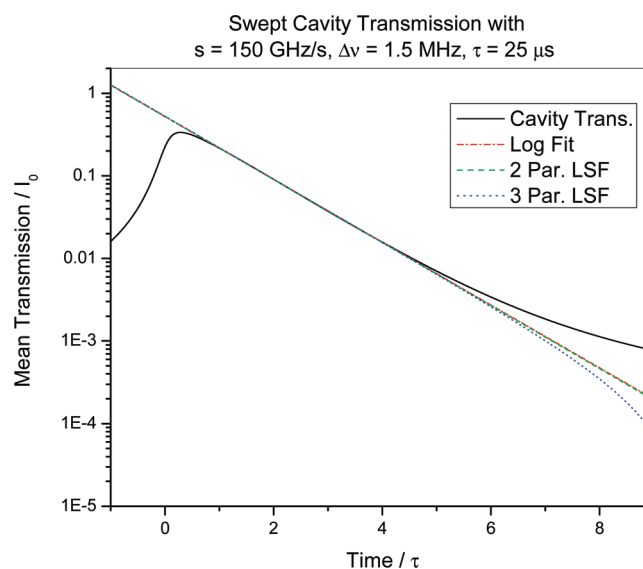


Figure 5. Calculated frequency swept mean cavity transmission, normalized to I_0 . The conditions are the same as those in Figure 4 except a larger fwhm line width of 1.5 MHz.

changing the ratio between trigger threshold and I_0 by 15% also makes the simulation in significantly worse agreement with the experiment. With wrong laser line width, adjusting the trigger threshold in the simulation will not produce a satisfactory fitting result. In Figure 2a, the small bump near 3 ms of the data curve that is not reproduced in the simulations is likely caused by the low-frequency excess jitter of the laser frequency, which can on some sweeps drive the laser back into near resonance with the cavity. With $s = 0.76$ GHz/s, 3 ms corresponds to a frequency sweep of 2.3 MHz, well within the long term jitter of the laser. For the faster sweep rate, this bump is not observed.

Bias and Uncertainty of k in Swept CRDS. Figures 4 and 5 show the calculated mean cavity transmission, by using eq 8, as a

Table 1. Simulations of Rapid Sweep of Laser with Frequency Noise over a High-Finesse Cavity, with Fits of the Transmission from the Fitting Range $1-4.5\tau$, after Passage through Resonance to an Exponential Decay^a

τ (μ s)	s (GHz/s)	$\Delta\nu_L$ (kHz)	log fit		2-par. LSF		3-par. LSF		mean amp (I_0)
			bias (% k)	$\sigma(k)$ (% k)	bias (% k)	$\sigma(k)$ (% k)	bias (% k)	$\sigma(k)$ (% k)	
25	1000	1500	-2.31	2.48	-1.99	2.94	-1.82	4.71	3.45×10^{-2}
25	1000	150	-0.238	0.724	-0.199	0.853	-0.177	1.33	3.61×10^{-3}
25	1000	15	-0.0250	0.440	-0.0179	0.507	-0.0132	0.795	4.94×10^{-4}
25	1000	1.5	-0.0035	0.155	-0.00064	0.177	0.00116	0.276	1.82×10^{-4}
25	1000	0.15	0.0011	0.0492	0.0010	0.0576	0.0024	0.090	1.51×10^{-4}
25	1000	0.015	0.0015	0.0079	0.0008	0.0092	0.0020	0.0142	1.47×10^{-4}
25	1000	0.00	0.0018	-	0.0012	-	0.0026	-	1.47×10^{-4}
25	500	1500	-4.24	3.21	-3.84	3.78	-3.66	6.41	6.85×10^{-2}
25	500	150	-0.450	1.06	-0.388	1.22	-0.356	1.96	7.22×10^{-3}
25	500	15.0	-0.0479	0.584	-0.0339	0.682	-0.0231	1.05	9.88×10^{-4}
25	500	1.50	-0.0071	0.221	0.0041	0.252	0.016	0.392	3.64×10^{-4}
25	500	0.15	0.0014	0.0655	0.0081	0.0766	0.0200	0.124	3.01×10^{-4}
25	500	0.015	0.0023	0.0110	0.0087	0.0131	0.0213	0.0206	2.95×10^{-4}
25	500	0.00	0.0027	-	0.0085	-	0.0205	-	2.93×10^{-4}
25	150	1500	-12.5	5.18	-12.1	6.48	-12.3	11.6	2.18×10^{-1}
25	150	150	-1.46	1.95	-1.28	2.27	-1.19	3.56	2.40×10^{-2}
25	150	15.0	-0.161	0.937	-0.121	1.12	-0.093	1.732	3.29×10^{-3}
25	150	1.50	-0.0288	0.373	-0.0041	0.434	0.0166	0.683	1.21×10^{-3}
25	150	0.15	-0.0013	0.126	0.0076	0.138	0.0274	0.217	1.00×10^{-3}
25	150	0.015	0.0030	0.0193	0.0103	0.0226	0.0308	0.0354	9.83×10^{-4}
25	150	0.00	0.0029	-	0.0088	-	0.0283	-	9.86×10^{-4}
25	50	1500	-30.2	7.24	-31.65	7.93	-35.96	26.6	5.55×10^{-1}
25	50	150	-4.20	3.16	-3.79	3.84	-3.58	6.49	7.13×10^{-2}
25	50	15.0	-0.490	1.31	-0.425	1.58	0.419	2.48	9.87×10^{-3}
25	50	1.50	-0.113	0.644	-0.191	0.740	-0.352	1.16	3.64×10^{-3}
25	50	0.15	-0.035	0.106	-0.173	0.123	-0.361	0.194	3.01×10^{-3}
25	50	0.015	-0.023	0.0337	-0.175	0.0393	-0.362	0.062	2.95×10^{-3}
25	50	0.00	-0.023	-	-0.174	-	-0.364	-	2.96×10^{-3}

^a τ is the cavity lifetime, s the sweep rate, and $\Delta\nu_L$ the full width at half-maximum of the laser. Least-squares fits to the ensemble of generated decay transients by Monte-Carlo simulation were used to determine the bias, uncertainty in k , and the transmission intensity at the beginning of each fit interval. The intensity is expressed in terms of I_0 , which is the mean cavity transmission if the laser is of fixed frequency and on-resonance with the cavity mode. The log fit is a least-squares fit of the log of the intensity vs time to a straight line, with slope k . For the two- and three-parameter fits, nonlinear least-squares fit to an exponential decay, $A \exp(kt) + B$ with a fixed ($B = 0$) or floating baseline, respectively, were done. The calculations of the standard deviations of k were done by fitting numerically simulated decays. Each simulation included 1000 sets of 25 transients, with the average of each set of 25 fitted. $\sigma(k)$ is the standard deviation of the ensemble of 1000 decay rates that result from the fit. Assuming these follow a χ^2 distribution, the standard error of these estimates will be 4.47% of their value.

function of time under two different assumptions. In Figure 4, we use parameters as reported in the work of He and Orr,¹³ where $\Delta\nu_L = 150$ kHz, $s = 150$ GHz/s, and $\tau = 25$ μ s. This laser line width reflects the use of an external cavity diode laser (ECDL). The decay is nearly exponential out to 8 time constants. For Figure 5, the assumed line width is changed to $\Delta\nu_L = 1.5$ MHz, which is a typical value for a DFB diode laser. Here, the distortions from a simply exponential decay are very pronounced and a unique decay rate is hard to define. The ECDL used by He and Orr is reported by them to have a Gaussian rather than Lorentzian spectrum.⁹ As a function of time after passing through resonance, the spectral overlap of a Gaussian spectrum with the resonant cavity mode will decrease faster in time than the cavity light injected at near resonance, and so the distortions of the decay will be insignificant as long as no other cavity modes cross resonance (TEM₀₀ or higher order transverse ones with significant spatial overlap with the input beam).

We have fit the calculated mean decay transients, by the model described above, to determine the cavity decay rate, as would be done in an experiment. One method, used the early CRDS work of O'Keefe and Deacon,¹ is to calculate the log of the cavity transmission, and then to perform an unweighted linear least-squares fit that to a straight line, which has slope k . Such a fit gives greater weight to the tail of the decay, where, as is evident from above, the decays deviate strongly from an exponential decay. We also performed nonlinear least-squares fits (LSF) of the calculated transmission values to an exponential decay $A \exp(-kt) + B$, as we do in our own experiments.⁸ For experiments dominated by detector noise, this gives the minimum dispersion in the value of k . We performed these fits as two-parameter fits where A and k were varied and $B = 0$ was assumed, as well as three-parameter fits with A , B , and k all fitting parameters.

With eq 20 we first attempted to do a nonlinear least-squares fit of each calculated transient to an exponential decay. In the

Table 2. Simulations of Rapid Sweep of Laser with Frequency Noise over a High-Finesse Cavity, with Fits of the Transmission from the Fitting Range $2-8\tau$, after Passage through Resonance to an Exponential Decay^a

τ (μ s)	s (GHz/s)	$\Delta\nu_L$ (kHz)	log fit		2-par. LSF		3-par. LSF		mean amp. (I_0)
			bias (% k)	$\sigma(k)$ (% k)	bias (% k)	$\sigma(k)$ (% k)	bias (% k)	$\sigma(k)$ (% k)	
25	1000	1500	-9.05	2.64	-2.53	2.75	-1.62	3.18	1.29×10^{-2}
25	1000	150	-1.16	0.915	-0.260	0.848	-0.162	0.963	1.33×10^{-3}
25	1000	15.0	-0.150	0.586	-0.0265	0.481	-0.0134	0.558	1.82×10^{-4}
25	1000	1.50	-0.040	0.206	-0.0026	0.173	0.00206	0.198	6.69×10^{-5}
25	1000	0.15	-0.0035	0.065	-0.00018	0.055	0.0037	0.0634	5.54×10^{-5}
25	1000	0.015	0.0032	0.021	0.000	0.0180	0.00389	0.021	5.42×10^{-5}
25	1000	0.00	0.0020	-	-0.00190	-	-0.00191	-	5.41×10^{-5}
25	500	1500	-12.6	3.29	-4.59	3.83	-3.24	4.50	2.61×10^{-2}
25	500	150	-1.78	1.21	-0.487	1.21	-0.333	1.39	2.66×10^{-3}
25	500	15.0	-0.229	0.583	-0.0515	0.679	-0.0317	1.056	3.63×10^{-4}
25	500	1.50	-0.0584	0.260	-0.0069	0.242	0.00033	0.279	1.34×10^{-4}
25	500	0.15	-0.0064	0.0839	-0.00217	0.0796	0.00383	0.091	1.11×10^{-4}
25	500	0.015	-0.0014	0.0258	0.0154	0.0250	0.0305	0.0288	1.07×10^{-4}
25	500	0.00	0.0022	-	-0.0036	-	0.0022	-	1.08×10^{-4}
25	150	1500	-25.4	3.98	-13.4	6.02	-10.0	7.36	8.97×10^{-2}
25	150	150	-5.02	2.024	-1.56	2.29	-1.11	2.65	8.92×10^{-3}
25	150	15.0	-0.702	1.07	-0.177	1.08	-0.117	1.25	1.21×10^{-3}
25	150	1.50	-0.185	0.367	-0.0434	0.449	-0.0270	0.724	4.46×10^{-4}
25	150	0.15	-0.0277	0.146	-0.0313	0.131	-0.0198	0.151	3.80×10^{-4}
25	150	0.015	-0.0058	0.0486	0.0218	0.0443	0.0602	0.0511	3.73×10^{-4}
25	150	0.00	0.0023	-	-0.0319	-	-0.0210	-	3.61×10^{-4}
25	50	1500	-41.2	4.40	-31.4	7.97	-25.6	-	2.75×10^{-1}
25	50	150	-12.1	2.96	-4.53	3.77	-3.26	4.44	2.71×10^{-2}
25	50	15.0	-2.02	1.46	-0.538	1.52	-0.361	1.76	3.64×10^{-3}
25	50	1.50	-0.553	0.718	-0.156	0.709	-0.115	0.823	1.33×10^{-3}
25	50	0.150	-0.0914	0.180	-0.124	0.175	-0.0992	0.201	1.11×10^{-3}
25	50	0.015	-0.0052	0.080	-0.121	0.079	-0.0979	0.0915	1.08×10^{-3}
25	50	0.00	0.0032	-	-0.122	-	-0.100	-	1.08×10^{-3}

^a τ is the cavity lifetime, s the sweep rate, and $\Delta\nu_L$ the full width at half-maximum of the laser. Least-squares fits to the ensemble of generated decay transients by Monte-Carlo simulation were used to determine the bias, uncertainty in k , and the transmission intensity at the beginning of each fit interval. The intensity is expressed in terms of I_0 , which is the mean cavity transmission if the laser is of fixed frequency and on-resonance with the cavity mode. The log fit is a least-squares fit of the log of the intensity vs time to a straight line, with slope k . For the two- and three-parameter fits, nonlinear least-squares fit to an exponential decay, $A \exp(kt) + B$ with a fixed ($B = 0$) or floating baseline, respectively, were done. The calculations of the standard deviations of k were done by fitting numerically simulated decays. Each simulation included 1000 sets of 25 transients, with the average of each set of 25 fitted. $\sigma(k)$ is the standard deviation of the ensemble of 1000 decay rates that result from the fit. Assuming these follow a χ^2 distribution, the standard error of these estimates will be 4.47% of their value.

simulation, a time step of $t_r = 2$ ns was used. However, if $\Delta\nu_L$ is larger than 150 kHz, some of the transients were found to have such high noise or even have already decayed away before reaching the fitting range (over the time interval $1-4.5\tau$ or $2-8\tau$ after passage through resonance, as used by He and Orr^{9,12,13}) that the fits became unstable, generating even some negative k fit values (which generated overflow errors) or near zero k . Instead, we averaged successive groups of 25 simulated cavity transmission transients. Each one of these was fit to an exponential decay in the time range first $1-4.5\tau$ and then $2-8\tau$ after resonance, and ensembles of $N_f = 1000$ such group fit results were analyzed to obtain the bias and uncertainty of the extracted k . Simulations are reported with $\Delta\nu_L$ spanning 15 Hz to 1.5 MHz, and s spanning 50–1000 GHz/s. τ was fixed at 25 μ s. The results are a function only of the “reduced” values of $\Delta\nu_L\tau$ and $s\tau^2$. The 1σ error bar for k is smaller than $\sigma(k)$ by a factor of $(2/(N_f - 1))^{1/2}$, given that a χ^2 distribution in $N_f - 1$ degrees of freedom has a standard

deviation of $(2(N_f - 1))^{1/2}$. The rms fluctuations in k are on the order of 1% despite the averaging of 25 decays. This noise in the fitted k also decays rather slowly as the laser line width is reduced, by only a factor of ≈ 46 when the $\Delta\nu_L$ is reduced by a factor of 10^4 . In the limit of small $\Delta\nu_L$ values (such that $\exp(i(\phi(t) - \phi(t'))) \approx 1 + i(\phi(t) - \phi(t'))$) and linear error propagation can be used, it can be shown that the standard deviation of the fitted k value will be proportional to $\Delta\nu_L$. The standard error for the bias is $\sigma(k)/(1000)^{1/2}$. It should be noted that for large fluctuations (large $\Delta\nu_L$), the bias in the fit to the mean transmission function does not match the bias extracted from a large number of fits to decays with noise. This reflects the break down of the linear error propagation expressions.

The results of these fits are presented in Tables 1 and 2. We report the bias in k , which is the fractional difference in the value of k returned from the least-squares fit from the value of k used to produce the simulation. In most cases, the bias is negative; i.e.,

Table 3. Calculated Bias, with Three Fitting Methods for Both Fitting Ranges, in k with the Mean Transmission from Eqs 15 and 19 of Approximate Integration Method^a

τ (μ s)	s (GHz/s)	$\Delta\nu_L$ (kHz)	fitting range 1–4.5 τ			fitting range 2–8 τ		
			log fit bias (% k)	2-par. LSF bias (% k)	3-par. LSF bias (% k)	log fit bias (% k)	2-par. LSF bias (% k)	3-par. LSF bias (% k)
25	1000	1500.	−2.14	−1.93	−1.83	−6.90	−2.30	−1.65
25	1000	150	−0.220	−0.195	−0.183	−0.821	−0.235	−0.168
25	1000	15	−0.0223	−0.0199	−0.0193	−0.0838	−0.0235	−0.0167
25	1000	1.5	−0.00255	−0.00323	−0.00477	−0.00491	−0.00195	−0.00110
25	1000	0.15	0.00152	−0.00162	−0.00345	0.0186	2.72×10^{-4}	5.56×10^{-4}
25	1000	0.015	0.00207	−0.00146	−0.00332	0.0228	4.95×10^{-4}	7.23×10^{-4}
25	1000	0.00	-9.83×10^{-5}	-3.45×10^{-4}	8.72×10^{-4}	7.06×10^{-5}	−0.00295	-4.21×10^{-4}
25	500	1500	−4.17	−3.82	−3.67	−11.9	−4.47	−3.24
25	500	150	−0.439	−0.389	−0.366	−1.61	−0.469	−0.335
25	500	15.0	−0.0442	−0.0376	−0.0334	−0.167	−0.0470	−0.0334
25	500	1.50	−0.00429	2.30×10^{-4}	0.00570	−0.00979	−0.00343	−0.00154
25	500	0.15	0.00396	0.00420	0.0100	0.0372	0.00111	0.00192
25	500	0.015	0.00509	0.00460	0.0105	0.0457	0.00157	0.00227
25	500	0.00	7.49×10^{-4}	6.84×10^{-3}	0.0189	1.88×10^{-4}	−0.00531	-1.23×10^{-7}
25	150	1500	−12.4	−12.1	−12.3	−25.3	−13.4	−10.0
25	150	150	−1.44	−1.29	−1.22	−4.88	−1.54	−1.11
25	150	15.0	−0.148	−0.130	−0.123	−0.552	−0.158	−0.113
25	150	1.50	−0.0158	−0.0137	−0.0142	−0.0331	−0.0240	−0.0230
25	150	0.15	0.0117	−0.00206	−0.00344	0.125	−0.0118	−0.0157
25	150	0.015	0.0154	-8.91×10^{-4}	−0.00237	0.474	−0.0550	−0.0782
25	150.	0.00	9.41×10^{-4}	0.00650	0.0255	2.02×10^{-4}	−0.0335	−0.0227
25	50	1500	−30.2	−31.6	−36.0	−41.2	−31.4	−25.6
25	50	150	−4.17	−3.82	−3.67	−11.9	−4.47	−3.24
25	50	15.0	−0.449	−0.450	−0.505	−1.61	−0.474	−0.342
25	50	1.50	−0.0707	−0.215	−0.438	−0.0997	−0.0902	−0.0951
25	50	0.15	0.00801	−0.200	−0.450	0.383	−0.0581	−0.0796
25	50	0.015	0.0189	−0.199	−0.451	0.474	−0.0550	−0.0782
25	50	0.00	−0.0248	−0.176	−0.367	9.50×10^{-4}	−0.124	−0.101

^a For zero line width situations, the mean transmission is calculated from eq 13.

the fitted k value is less than the one used to generate the data, which is easily predicted by looking at the deviation from an exponential decay evident in Figures 4 and 5. In both tables, we report the mean amplitude, A (cavity transmission at the start of the fitted interval), in units of I_0 for each condition and fitting range. For comparison, we also report the bias calculated with the mean transmission by eqs 15 and 19 of approximate integration method for each condition. The calculated bias is displayed in Table 3, corresponding to three fitting methods for both fitting ranges, respectively. For zero line width cases, the part before “ \approx ” of eq 13 is used. The time step for this calculation is 1 ns, half of t_r . No uncertainty can be calculated with those equations.

We can now compare the expected signal-to-noise levels for a CRDS experiment done using a light intensity modulator versus simply sweeping through resonance. Because of the need to rapidly tune through resonance in the latter case, the light intensity on the detector is reduced substantially (by about 2 orders of magnitude for the parameters reported by He and Orr¹³) versus what one would have with the same cavity and laser without sweeping (or a very slow sweep restricted to a range close to resonance). This, by itself, translates into a corresponding reduction in predicted sensitivity. In cases where the detector

noise dominates, the noise in k is inversely proportional to the light intensity on the detector. At higher power, where shot noise dominates, the CRDS sensitivity is inversely proportional to the square root of the light intensity. Reducing the time delay after resonance for the start of the fit to the transient will increase its amplitude (up to 7.4 times for zero delay) but will introduce increased bias and noise due to laser frequency jitter and the highly oscillatory term as represented in eq 19. In addition, the interference of the driving laser radiation and the light stored in the cavity produces noise on the detector, which leads to noise in the extracted cavity decay rates, even if one had no detector noise. Even for the narrow line width laser of $\Delta\nu_L = 150$ kHz, after averaging 4000 decays (corresponding to 1 s),¹³ a laser phase jitter induced noise of 0.21% per $\text{Hz}^{1/2}$ in k is predicted, or converted into sample absorbance units for $k = 4 \times 10^4 \text{ s}^{-1}$, a noise of $3 \times 10^{-9} \text{ cm}^{-1} \text{ Hz}^{-1/2}$.

In their most recent paper, He and Orr¹³ report a noise in the absorption coefficient of the sample of $5 \times 10^{-10} \text{ cm}^{-1} \text{ Hz}^{-1/2}$, which is 2 times worse than the single-shot sensitivity, $2.5 \times 10^{-10} \text{ cm}^{-1}$,²⁸ of our light switch-off cw-CRDS setup, or an order of magnitude worse per $\text{Hz}^{1/2}$. If we use their reported line width of 150 kHz in our simulation, we predict a noise in k that is

6 times higher than He and Orr's reported value. Our model is not directly applicable to their experiment because the dominant broadening of an ECDL is technical noise with a Gaussian spectrum. The literature suggests that the Lorentzian component of an external diode laser should be smaller, a few kilohertz.^{29,30} Wyatt²⁹ reported that the phase diffusion line width of their ECDL was calculated to be 2 kHz using a modified Schawlow–Townes model, which attributes the phase noise to spontaneous emission. Ignoring the Gaussian technical noise, our simulations with a Lorentzian line width of 1.5 kHz should be applicable to the swept cavity CRDS using an ECDL. Our simulations predict that reducing the Lorentzian line width from 150 to 1.5 kHz should reduce the noise in the extracted k by a factor of ≈ 5 . This brings our prediction, 3.9×10^{-10} , 4.6×10^{-10} , and $7.2 \times 10^{-10} \text{ cm}^{-1} \text{ Hz}^{-1/2}$, for the linearized, two-parameter and three-parameter least-squares fit. Our simulation results are in excellent agreement with the noise level reported by He and Orr, $5 \times 10^{-10} \text{ cm}^{-1} \text{ Hz}^{-1/2}$, which suggests that the phase noise in the ECDL is likely a major contributing factor in the sensitivity limit of their instrument, i.e., that they have reached practical theoretical detection limit given their mirrors and lasers.

Finally, we point out one difference between swept frequency and swept cavity CRDS. In swept cavity CRDS, the incident laser frequency is fixed during the whole sweep. However, the frequency of the intracavity field changes with time because of the Doppler shift from multiple reflections on the moving cavity mirror. The intracavity field remains in-resonance with the cavity mode during the sweeping because the Doppler shift compensates for the mode shift from the cavity length change. Therefore, the absorbent in the cavity is sampled by a frequency changing light source, which will introduce a small error in the detection. For a sweep corresponding to a rate 150 GHz/s and with $\tau = 25 \mu\text{s}$, the frequency shift during one τ period is about 4 MHz, which is much larger than the cavity mode width. This is much less than thermal Doppler widths but could be important in sub-Doppler spectroscopy experiments.³¹ In swept frequency CRDS, on the contrary, the light that enters the cavity is all near the cavity resonance and thus at fixed frequency.

CONCLUSION

The purpose of this article is to assess the sensitivity limit of the swept cavity CRDS. Concurrently, we have developed a model of the excitation of a high-finesse cavity by a linearly frequency swept laser with finite line width. Compared with previous studies,^{18,20} we have derived the averaged cavity transmitted intensity in the excitation both as exact sum-overpasses method and as approximate analytical integrals. For the second method, an approximate but computationally more efficient stationary phase approximation expression is also derived. The calculated peak values of the mean cavity transmission matches very well with the measured ones. When this mean transmission waveform is used to extract the cavity decay rate with three different fitting models, a negative bias of k exists because the waveform decays as an inverse second power at long time, slower than exponential decay.

To obtain statistical fluctuations in the cavity decay rate k , recursive relation eq 20, exact but more time-consuming, and eq 21, approximate but with higher calculation efficiency, have been derived for the numerical simulation of each transmitted waveform. The mean transmitted waveforms were averaged from those crossing a threshold detector voltage, among all single-sweep

transmitted waveforms, are shown in the Figures 2a and 3a. These are well reproduced by the Monte Carlo simulations, which were processed in the same way. With eq 20, for a range of parameters spanning those likely to be encountered in real experiments,¹³ numerical results demonstrate that the theoretical signal-to-noise ratio and thus sensitivity of swept cavity (or equivalently, frequency) CRDS is substantially below that for CRDS where one attenuates the laser either with current modulation or with an external modulator.

This work clearly demonstrates that swept cavity CRDS will give a very poor sensitivity if one uses a DFB or FP diode laser to excite the cavity. In agreement with the experimental results of He and Orr, the method can give good sensitivity when a low phase noise external cavity diode laser is used to excite the cavity because of the 3 orders of magnitude drop in the Lorentzian contribution to the laser line width. It is worth noting that the cost of such external cavity lasers is approximately 1 order of magnitude higher than a DFB laser and they are far less robust with respect to vibrations and other environmental disturbances. This extra cost swamps the cost savings of not requiring an optical switch. The theoretical limit of the swept cavity CRDS method, even when a narrow line width ECDL is used for excitation, is below what we routinely obtain using a DFB diode laser to excite the cavity. When a cavity is excited with a 25 μs decay time with an ECDL, assuming zero line width, in switch-off cw-CRDS experiments, the cavity transmission is much higher than with a DFB laser, by a factor of $(1 + 2\pi\Delta\nu_L\tau) = 158$ for $\tau = 25 \mu\text{s}$ and $\Delta\nu_L = 1 \text{ MHz}$. This translates into a dramatic improvement of signal-to-noise, such that the decay should be largely shot-noise-limited. Assuming a peak power on the detector of 1 mW at the start of a ring-down, the shot-noise limited decay of the cavity would give a sensitivity of $3 \times 10^{-12} \text{ cm}^{-1}$ per shot.^{7,8}

AUTHOR INFORMATION

Corresponding Author

*E-mail: lehmann@virginia.edu.

ACKNOWLEDGMENT

This work is supported by the National Science Foundation and the University of Virginia.

REFERENCES

- (1) O'Keefe, A.; Deacon, D. A. G. *Rev. Sci. Instrum.* **1988**, *59*, 2544–2551.
- (2) Scherer, J. J.; Paul, J. B.; Collier, C. P.; O'Keefe, A.; Rakestraw, D. J.; Saykally, R. J. *Spectroscopy* **1996**, *11*, 46–50.
- (3) Busch, K. W.; Busch, M. A., Eds. *Cavity Ringdown Spectroscopy: An Ultratrace-Absorption Measurement Technique*; ACS Symposium Series 720; Oxford: Washington, DC, 1999.
- (4) Berden, G.; Peeters, R.; Meijer, G. *Int. Rev. Phys. Chem.* **2000**, *19*, 565–607.
- (5) Vallance, C. *New J. Chem.* **2005**, *29*, 867–874.
- (6) Hodges, J. T.; Ciurylo, R. *Rev. Sci. Instrum.* **2005**, *76*, 023112.
- (7) Romanini, D.; Lehmann, K. K. *J. Chem. Phys.* **1993**, *99*, 6287–6301.
- (8) Lehmann, K. K.; Huang, H. In *Frontiers of Molecular Spectroscopy*; Laane, J., Ed.; Elsevier: Amsterdam, 2008; Chapter 18, pp 623–658.
- (9) He, Y.; Orr, B. J. *Chem. Phys. Lett.* **2000**, *319*, 131–137.
- (10) He, Y.; Orr, B. J. *Appl. Phys. B: Laser Opt.* **2002**, *75*, 267–280.
- (11) He, Y.; Orr, B. J. *Appl. Phys. B: Laser Opt.* **2004**, *79*, 941–945.

- (12) He, Y.; Orr, B. J. *Appl. Opt.* **2005**, *44*, 6752–6761.
- (13) He, Y.; Orr, B. J. *Appl. Phys. B: Laser Opt.* **2006**, *85*, 355–364.
- (14) Ioannidis, Z. K.; Radmore, P. M.; Giles, I. P. *Opt. Lett.* **1988**, *13*, 422–424.
- (15) Li, Z. Y.; Bennett, R. G. T.; Stedman, G. E. *Opt. Commun.* **1991**, *86*, 51–57.
- (16) Li, Z.; Stedman, G. E.; Bilger, H. R. *Opt. Commun.* **1993**, *100*, 240–246.
- (17) An, K. W.; Yang, C. H.; Dasari, E. E.; Feld, M. S. *Opt. Lett.* **1995**, *20*, 1068–1070.
- (18) Poirson, J.; Bretenaker, F.; Vellet, M.; Floch, A. L. *J. Opt. Soc. Am. B* **1997**, *14*, 2811–2817.
- (19) Bakowski, B.; Corner, L.; Hancock, G.; Kotchie, R.; Peverall, R.; Ritchie, G. A. D. *Appl. Phys. B: Laser Opt.* **2002**, *75*, 745–750.
- (20) Morville, J.; Romanini, D.; Chenevier, M.; Kachanov, A. A. *Appl. Opt.* **2002**, *41*, 6980–6990.
- (21) Romanini, D.; Gambogi, J.; Lehmann, K. K. Cavity Ring-Down Spectroscopy with CW Diode Laser Excitation. Talk RH06 in 50th International Symposium of Molecular Spectroscopy, Columbus, OH, 1995.
- (22) Romanini, D.; Kachanov, A. A.; Sadeghi, N.; Stoeckel, F. *Chem. Phys. Lett.* **1997**, *264*, 316–322.
- (23) Huang, H.; Lehmann, K. K. *Appl. Phys. B: Laser Opt.* **2009**, *94*, 355–366.
- (24) Hahn, J. W.; Yoo, Y. S.; Lee, J. Y.; Kim, J. W.; Lee, H. W. *Appl. Opt.* **1999**, *38*, 1859–1866.
- (25) Dumeige, Y.; Trebaol, S.; Ghisa, L.; Nguyen, T. K. N.; Tavernier, H.; Feron, P. *J. Opt. Soc. Am. B* **2008**, *25*, 2073–2080.
- (26) Henry, C. H. *IEEE J. Quantum Electron.* **1982**, *QE-18*, 259–264.
- (27) Dudek, J. B.; Tarsa, P. B.; Velasquez, A.; Wladyslawski, M.; Rabinowitz, P.; Lehmann, K. K. *Anal. Chem.* **2003**, *75*, 4599–4605.
- (28) Huang, H.; Lehmann, K. K. *Appl. Opt.* **2010**, *49*, 1378–1387.
- (29) Wyatt, R.; Devlin, W. J. *Electron. Lett.* **1983**, *19*, 110–112.
- (30) van Exter, M. P.; Kuppens, S. J. M.; Woerdman, J. P. *IEEE J. Quantum Electron.* **1992**, *28*, 580–584.
- (31) Lisak, D.; Hodges, J. T. *Appl. Phys. B: Laser Opt.* **2007**, *88*, 317–325.